



Published in final edited form as:

Sci Signal. ; 10(500): . doi:10.1126/scisignal.aak9741.

Foxo1 and Foxp1 play opposing roles in regulating the differentiation and antitumor activity of T_H9 cells programmed by IL-7

Enguang Bi^{1,*}, Xingzhe Ma^{1,*}, Yong Lu^{1,*}, Maojie Yang¹, Qiang Wang¹, Gang Xue¹, Jianfei Qian¹, Siqing Wang², and Qing Yi^{1,†}

¹Department of Cancer Biology, Lerner Research Institute, Cleveland Clinic, Cleveland, OH 44195, USA

²Department of Cancer Immunology, Institute of Translational Medicine, The First Hospital of Jilin University, Changchun 130061, China

Abstract

Tumor-specific CD4⁺ T helper 9 (T_H9) cells, so-called because of their production of the cytokine interleukin-9 (IL-9), are a powerful effector T cell subset for cancer immunotherapy. We found that pretreatment of naïve CD4⁺ T cells with IL-7 further enhanced their differentiation into T_H9 cells and augmented their antitumor activity. IL-7 markedly increased the abundance of the histone acetyltransferase p300 by activating the STAT5 and PI3K-AKT-mTOR signaling pathways and promoting the acetylation of histones at the *Il9* promoter. As a result, the transcriptional regulator Foxo1 was dephosphorylated and translocated to the nucleus, bound to the *Il9* promoter, and induced the production of IL-9 protein. In contrast, Foxp1, which bound to the *Il9* promoter in naïve CD4⁺ T cells and inhibited *Il9* expression, was outcompeted for binding to the *Il9* promoter by Foxo1 and translocated to the cytoplasm. Furthermore, forced expression of Foxo1 or a deficiency in Foxp1 in CD4⁺ T cells markedly increased the production of IL-9, whereas a deficiency in Foxo1 inhibited the ability of IL-7 to enhance the differentiation and antitumor activity of T_H9 cells. Thus, we identified the roles of Foxo1 as a positive regulator and Foxp1 as a negative regulator of T_H9 cell differentiation and antitumor activity, which may provide potential targets for cancer immunotherapy.

[†]Corresponding author. yiq@ccf.org.

*These authors contributed equally to this work.

SUPPLEMENTARY MATERIALS

www.sciencesignaling.org/cgi/content/full/10/500/eaak9741/DC1

Author contributions: Q.Y. and E.B. initiated the study, designed the experiments, and wrote the paper. E.B. performed most of the experiments and statistical analyses. X.M. did the Western blotting, confocal microscopy, and luciferase experiments. Y.L. helped with the animal experiments. Y.L. and X.M. read and edited the manuscript. M.Y. assisted in generating the transgenic mice. Q.W., G.X., S.W., and J.Q. provided critical suggestions.

Competing interests: The authors declare that they have no competing interests.

Data and materials availability: Microarray data accession number is GSE86542.

INTRODUCTION

Naïve CD4⁺ T cells exit from quiescent status, become activated, and differentiate into different T helper (T_H) cell subsets upon antigen stimulation in the presence of certain cytokines, including T_H1, T_H2, T_H9, T_H17, regulatory T (T_{reg}) cells, and follicular helper T (T_{FH}) cells, to mediate various immune responses (1). The cytokine interleukin-9 (IL-9) was previously considered to be a T_H2-type cytokine and related to the T_H2-type immune response (2). Although it was found that IL-4, together with transforming growth factor- β (TGF- β), stimulates activated T cells to produce IL-9 more than 20 years ago (3), this population of T_H cells was only relatively recently identified as a specific subset called T_H9 cells (4), and two transcriptional regulators that directly bind to the *Il9* promoter [PU.1 and IRF4 (interferon regulatory factor 4)] were identified (5, 6). In addition to T_H2 cell-like functions such as mediating allergic inflammation (7) and clearing intestinal parasites (8), the most prominent function of T_H9 cells is their antitumor activity, especially against melanoma (9, 10). We and others showed that T_H9 cells produce IL-9 and IL-21 to activate the antitumor function of CD8⁺ cytotoxic T cells (10, 11). Although transcriptional regulators [including PU.1, IRF4, GATA3, STAT5 (signal transducer and activator of transcription 5), and IRF1] are involved in regulating the differentiation of naïve CD4⁺ T cells into T_H9 cells (4–6, 11, 12), T_H9 cell-specific transcriptional factors are still unknown. It is unclear how the expression of *Il9* is negatively regulated during T_H9 cell differentiation.

IL-7 signaling is critical for thymocyte development, naïve T cell survival, and homeostasis in vivo (13). When normal mice are injected with IL-7, the number of T cells increases in peripheral lymph nodes. In addition, in mice that are irradiated in preparation for bone marrow transfer or rendered lymphopenic by cyclophosphamide, IL-7 accelerates T cell accumulation in peripheral lymph organs (14–16). Those features of IL-7 make it attractive for cancer therapy because many cancer patients experience cytotoxic chemotherapy-induced lymphopenia. When IL-7 is administered in vivo, it promotes T_H1 cell differentiation and a T cell-dependent antitumor reactivity (17–20). In vitro, IL-7 prevents T cell death by increasing the abundance of the anti-apoptotic protein Bcl2 (21), which enables the increased numbers of T cells to be generated ex vivo for adoptive immunotherapy. The IL-7 receptor (IL-7R) consists of two subunits, the IL-7R α chain (IL-7Ra; also known as CD127) and the common γ chain (γ C; also known as CD132). The main signaling pathways induced by IL-7 are mediated by STAT5, the serine and threonine kinases PI3K (phosphatidylinositol 3-kinase) and AKT, and the mitogen-activated protein kinase ERK (extracellular signal-regulated kinase). Both the STAT5 and PI3K-AKT pathways are indispensable for cell survival (22, 23).

Here, we found that IL-7-treated CD4⁺ T cells exhibit enhanced T_H9 cell differentiation (hereafter referred to as IL-7-T_H9 cells) and antitumor activity compared to T_H9 cells that underwent differentiation in the absence of IL-7. Signaling of the IL-7R, including the STAT5 and PI3K-AKT-activated mTOR (mammalian target of rapamycin) pathways, was involved in histone acetylation at the *Il9* promoter. The transcription factors Foxo1 (Forkhead box protein O1) and Foxp1 (Forkhead box protein P1) played reciprocal roles in regulating T_H9 and IL-7-T_H9 cell differentiation. We conclude that the enhanced antitumor function of IL-7-pretreated T_H9 cells is Foxo1-dependent.

RESULTS

Pretreatment of naïve CD4⁺ T cells with IL-7 enhances their differentiation into T_H9 cells

To evaluate the effect of IL-7 on T_H9 cell differentiation, we cultured murine CD4⁺ T cells under T_H9-polarizing conditions [that is, in the presence of the cytokines IL-4 and TGF- β , and a monoclonal antibody (mAb) against interferon- γ (IFN- γ)] with or without IL-7. We found that IL-7 did not enhance T_H9 cell differentiation (fig. S1A), that is, the number of IL-9-expressing cells was not increased, which is consistent with a previous report (12). Considering the role of IL-7 in T cell homeostasis and survival, CD4⁺ T cells were pretreated with IL-7 for 48 hours and then cultured under T_H9-polarizing conditions. The number of IL-9- and IL-21-producing cells (T_H9 cells) was markedly increased in an IL-7 dose-dependent manner compared with cells that did not receive IL-7 pretreatment. Analysis by flow cytometry to measure the mean fluorescence intensity (MFI) of IL-9 in these cells confirmed these results (Fig. 1B). The enhanced generation of T_H9 cells was also confirmed by IL-9-specific enzyme-linked immunosorbent assay (ELISA) and real-time polymerase chain reaction (PCR) analyses (Fig. 1, C and D). However, when CD4⁺ T cells were pretreated with other common γ C receptor family cytokines, such as IL-2 or IL-15, T_H9 cell differentiation was not enhanced (Fig. 1E). These data suggest that IL-7 exerts a specific effect on T_H9 cell differentiation.

To explore whether IL-7 also enhanced the differentiation of human naïve CD4⁺ T cells into T_H9 cells, we conducted similar experiments and confirmed that IL-7 pretreatment also facilitated the generation of human T_H9 cells (fig. S1, B and C), suggesting that it is possible to generate human polarized T_H9 cells ex vivo for testing in clinical trials. The expression of *Il9* was rapidly and markedly induced on day 2 of differentiation and suddenly decreased on day 4 in T_H9 cells; however, in IL-7-T_H9 cells, *Il9* expression was substantially increased. A similar result was observed for *Il21* expression (Fig. 1D). To understand the features of IL-7-T_H9 cells, we performed a gene expression microarray to analyze T_H9-related genes. Although no new potential T_H9 cell-related transcription factors were identified (Fig. 1F), the abundances of T_H9 cytokines, including IL-9, IL-21, IL-10, and IL-2, were increased, indicative of enhanced T_H9 cell differentiation.

IL-7-T_H9 cells have enhanced antitumor activity

To investigate whether IL-7-T_H9 cells had enhanced antitumor function compared to normal T_H9 cells, we used both prophylactic and therapeutic models. In the prophylactic model, C57BL/6 mice were challenged with B16-OVA (ovalbumin) melanoma cells by intravenous injection, which was followed by the adoptive transfer of T_H cells on the same day. Lung metastasis was assessed on day 14 after tumor challenge (Fig. 2A). Consistent with our previous report (10), mice treated with T_H9 cells had a decreased tumor burden compared to those that received T_H1 cells (Fig. 2, B and C). Notably, IL-7-T_H9 cells exhibited enhanced antitumor function; lung tumors were almost cleared in all of the mice by day 14 (Fig. 2, B and C). We found that more donor CD4⁺ T cells were in the lung tissue of mice that received IL-7-T_H9 cells (Fig. 2D) than of those that received T_H1 or T_H9 cells, suggesting that IL-7-T_H9 cells were more persistent in vivo. The numbers of CD8⁺ T cells were also increased in the lung tissue of mice that received IL-7-T_H9 cells (Fig. 2E).

To determine whether these CD4⁺ T cells secreted IL-9 or other cytokines, donor-derived CD4⁺ T cells were sorted from the lung lymph nodes of the recipient mice and restimulated ex vivo with phorbol 12-myristate 13-acetate (PMA) and ionomycin, and the cell culture medium was collected for analysis by ELISA. We found that the IL-7-T_H9 cells secreted more IL-9 and IL-21 than did the T_H9 cells (Fig. 2, F and G). Moreover, in a therapeutic model, in which B16-OVA tumors were allowed to establish for 4 days before T cells were transferred into the mice (Fig. 2H), the IL-7-T_H9 cells also exhibited a substantially greater antitumor function than did the T_H9 cells. To investigate whether the enhanced antitumor function of the IL-7-T_H9 cells was dependent on IL-9 or IL-21, neutralizing antibodies against either IL-9 or IL-21R were injected into the mice. Blocking IL-9 in vivo substantially inhibited the antitumor effect of both T_H9 and IL-7-T_H9 cells (Fig. 2I). Blocking IL-21R in vivo partially reduced the antitumor activity of the IL-7-T_H9 cells but did not substantially affect the T_H9 cells.

It has been reported that IL-7 alone or in combination with other drugs exhibits therapeutic effects in mouse tumor models, but it is not known whether IL-7 can stimulate IL-9 production in tumor models in vivo. To explore this question, we used the B16 tumor model. C57BL/6 mice were injected with B16 tumor cells and received IL-7 or PBS from that same day for a further 14 days. IL-7 exhibited a substantial antitumor effect (fig. S2A), and this effect was associated with the increased amounts of *Il9* and *Il21* mRNAs in the tumor bed (fig. S2, B and C), suggesting that IL-7 stimulates IL-9 and IL-21 production in vivo. To examine whether CD4⁺ T cells secreted these cytokines in response to IL-7, total CD4⁺ T cells were isolated from the lung lymph nodes of PBS- or IL-7-treated B16-bearing mice and restimulated ex vivo with PMA and ionomycin. IL-7 stimulated the CD4⁺ T cells to secrete IL-9 and IL-21 (Fig. 2, J and K). To determine whether the anti-tumor effect of IL-7 was dependent on IL-9 or IL-21, we used anti-IL-9 or anti-IL-21R antibodies in the presence or absence of IL-7 in the B16 tumor model. Blocking IL-9, but not IL-21R, in vivo not only rendered the mice more susceptible to developing lung melanoma but also compromised the antitumor effects of IL-7 (Fig. 2L).

IL-7 induces changes in the gene expression profile of CD4⁺ T cells

To understand the global effect of IL-7 on transcriptional regulation, we performed another gene microarray assay with naïve CD4⁺ T cells that were either untreated or treated with IL-7. IL-7 induced a global change in gene expression in these cells, with more than 4000 genes showing increased expression and 7000 genes showing decreased expression. Specifically, there was no difference between the two groups of cells in terms of the expression of genes involved in T cell-related transcriptional factors (Fig. 3A and fig. S3A), survival pathways, or metabolic pathways (fig. S3B). However, we found that the expression of more than two-thirds of the histone-encoding genes on the microarray was statistically significantly decreased in response to IL-7, which was suggestive of a marked change in chromatin structure to affect gene expression (fig. S4).

Because the expression of genes encoding the transcription factors required for T cell differentiation did not substantially change as a result of IL-7 exposure, we considered whether IL-7 might affect T_H9 cell differentiation by modifying chromatin structure and

gene locus accessibility, similar to a previous report on the TRG locus (24). Because histone modifications include methylation and acetylation (the latter is modified by histone acetyltransferases and acetylation facilitates gene expression), we analyzed whether there were changes in histone acetyltransferases in response to IL-7. The expression of some genes encoding histone acetyltransferases increased in IL-7-treated cells (fig. S5A). In addition, the abundances of GCN5 and p300 mRNA and proteins were also increased by IL-7, which resulted in an increase in total histone 3 (H3) acetylation (Fig. 3C), whereas total histone 4 (H4) acetylation did not change (Fig. 3, B and C). To understand whether histone acetylation occurred at the *Il9* promoter locus, we performed chromatin immunoprecipitation (ChIP) assays and detected increased H3 acetylation and H4 acetylation at the *Il9* (Fig. 3D) and *Il21* promoter regions (fig. S5B). Studies showed that the acetylation of H3 Lys⁹ (H3K9) is enhanced in T_H9 cells compared to that in other T_H subset cells (5, 6), and we found that total acetylation of H3K9 (Fig. 3C) and acetylation of H3K9 at the *Il9* promoter locus (Fig. 3D) were also increased in response to IL-7. To verify the importance of acetyltransferases in IL-7-induced T_H9 cell differentiation, we performed experiments with a p300 inhibitor. We found that p300 inhibition slightly inhibited T_H9 cell differentiation but substantially inhibited the increased T_H9 cell differentiation induced by IL-7 (Fig. 3, E and F). Because of the global effect of p300 inhibition, other genes affected by p300 may also contribute to the decreased differentiation of T_H9 cells.

The STAT5 and PI3K-AKT-mTOR signaling pathways contribute to histone acetylation on the *Il9* promoter

Our earlier results suggest that IL-7 signaling modifies histone acetylation and may facilitate the access of transcription factors to the *Il9* locus. How IL-7 controls histone acetylation in T cells is unclear. We found that signals downstream of IL-7, including PI3K-AKT, ERK, and STAT5, were activated, which is consistent with previous reports (23). A luciferase assay in 293T cells demonstrated that STAT5 bound directly to the *p300* promoter and promoted its transcription (Fig. 4B), suggesting that STAT5 might contribute to the increased p300 abundance observed in IL-7-treated cells. To verify whether STAT5 directly bound to the *p300* promoter in IL-7-treated CD4⁺ T cells, we performed a ChIP assay with an anti-STAT5 antibody. We found that IL-7 substantially increased the amount of STAT5 that bound to the *p300* promoter in CD4⁺ T cells (Fig. 4C). In T_H9 cells, increased amounts of STAT5 bound to the *Il9* promoter were also detected after IL-7 treatment (fig. S6A). Western blotting analysis showed that STAT5 was substantially phosphorylated in CD4⁺ T cells on day 2 in the presence, but not absence, of IL-7, whereas the amounts of phosphorylated STAT5 (pSTAT5) were similar in T_H9 cells with or without IL-7 pretreatment (fig. S6B). Moreover, the abundance of mTOR in CD4⁺ T cells increased after IL-7 treatment (Fig. 4A). Similarly to Foxo1, mTOR is a downstream target of the PI3K-AKT pathway.

Considering the importance of mTOR in T cell differentiation (25), we wondered whether IL-7-induced histone acetylation and increased T_H9 cell differentiation were also mTOR-dependent. Rapamycin, an mTOR complex 1 (mTORC1) inhibitor, inhibited histone acetylation at the *Il9* promoter region, suggesting that mTOR plays a role in IL-7-induced histone acetylation (Fig. 4D). Rapamycin also inhibited the IL-7-induced increase in p300 abundance (Fig. 4E). Furthermore, rapamycin inhibited T_H9 cell differentiation in both T_H9

cell and IL-7- T_H9 cell systems (Fig. 4, F and G), whereas the mTOR activator MHY1485 substantially promoted T_H9 cell differentiation (Fig. 4, H and I). Together, these data suggest that the PI3K-AKT-mTOR pathway is important for the differentiation of naïve $CD4^+$ T cells into T_H9 cells and that both the STAT5 and PI3K-AKT-mTOR signaling pathways contribute to histone acetylation at the *Il9* promoter region.

Foxo1 and Foxp1 play opposing roles in regulating IL-9 production

We next sought to determine which transcriptional factors directly regulated the differentiation of IL-7- T_H9 cells in addition to the marked chromatin modification. With the chromatin modification, we hypothesized that the binding of positive transcriptional factors to the *Il9* promoter would increase after IL-7 treatment, but IL-7 may decrease the binding of negative regulators to the *Il9* promoter. Informatics analysis revealed two adjacent conserved Forkhead box transcription factor-binding sites on the *Il9* promoter (Fig. 5A), and we detected both Foxo1 and Foxp1 during T_H9 cell differentiation. Both Foxo1 and Foxp1 were found in naïve $CD4^+$ T cells, and they increased in abundance during T_H9 cell differentiation (Fig. 5B). A study showed that Foxp1 inhibits *Il21* expression by directly binding to the *Il21* promoter (26). Because we found that *Il21* expression was increased in IL-7- T_H9 cells, we wondered whether Foxp1 also regulated *Il9* expression. Because Foxo1 is an important downstream target of PI3K-AKT-mTOR signaling and because Foxo1 and Foxp1 compete for binding to *Il7r* promoter to regulate IL-7 signaling in naïve T cells (27, 28), we hypothesized that Foxo1, Foxp1, or both might regulate *Il9* expression. ChIP assays demonstrated that both Foxo1 and Foxp1 could bind to the *Il9* promoter in naïve $CD4^+$ T cells (Fig. 5, C and D). We overexpressed Foxo1 or knocked down Foxp1 in preactivated $CD4^+$ T cells under T_H9 -polarizing conditions. Our results showed that Foxo1 overexpression substantially enhanced T_H9 cell differentiation (Fig. 5, E and F), which also occurred as a result of Foxp1 knockdown (Fig. 5, G and H). These results were confirmed in mice in which Foxp1 or Foxo1 was conditionally knocked out in $CD4^+$ T cells. T_H9 cell differentiation was decreased as a result of Foxo1 deficiency (Fig. 5, I and J) but was substantially enhanced in Foxp1-deficient $CD4^+$ T cells (Fig. 5, K and L).

To further test our hypothesis that Foxo1 and Foxp1 oppositely and competitively regulated *Il9* expression in a direct manner, we performed an *Il9* promoter luciferase assay. Foxo1 alone only slightly increased *Il9* transcription (Fig. 5M); however, together with p300, Foxo1 substantially induced *Il9* transcription, which was markedly inhibited by Foxp1 (Fig. 5M). To confirm whether Foxo1 and Foxp1 bound to the predicted sites on the *Il9* promoter, promoters with point mutations were synthesized and used for luciferase assay. Both site 1 and site 2 were important binding sites for Foxo1 and Foxp1, because mutation of either site abolished the transcriptional activity of Foxo1 (Fig. 5N). Because Foxo family members in T cells include Foxo1, Foxo3, and Foxo4 and they have redundant functions in T cell regulation, we wondered whether Foxo3 and Foxo4 also played a role in T_H9 cell differentiation. We found that Foxo4 directly activated *Il9* transcription as determined with an *Il9* promoter luciferase assay (fig. S7A). In addition, the abundance of Foxo4 increased during T_H9 cell differentiation (fig. S7B). Ectopic over-expression of Foxo4 substantially increased T_H9 cell differentiation (fig. S7, C and D), whereas Foxo4 deficiency in $CD4^+$ T cells diminished T_H9 cell differentiation (fig. S7, E and F). Furthermore, we found that

Foxo4 bound to the *Il9* promoter and became localized to the nucleus in response to IL-7 (fig. S7, G and H). Thus, these data suggest that Foxo1 and Foxp1 are transcriptional regulators that modulate T_H9 cell differentiation in a reciprocal manner.

Foxo1 and Foxp1 have reciprocal roles in the enhancement of IL-7–T_H9 cell differentiation and antitumor activity

To verify whether Foxo1 and Foxp1 were also involved in enhanced differentiation of IL-7–T_H9 cells, we first examined whether IL-7 affected the binding of Foxo1 or Foxp1 to the *Il9* promoter. We found that IL-7 increased the amount of Foxo1 that bound to the *Il9* promoter, whereas it increased the dissociation of bound Foxp1 from the *Il9* promoter (Fig. 6A). IL-7 treatment did not substantially change the abundances of Foxo1 or Foxp1 mRNAs in T_H9 cells (fig. S8A) but slightly increased the abundance of Foxo1 protein (Fig. 6B).

Furthermore, the abundance of pFoxo1 was decreased in response to IL-7, suggesting that Foxo1 had increased nuclear localization and transcriptional activity. Confocal microscopy confirmed that IL-7 increased the amount of Foxo1 in the nucleus in CD4⁺ T cells (Fig. 6C). IL-7 signaling also did not affect the abundance of Foxp1 protein (Fig. 6B), but most of the nuclear Foxp1 protein was exported into the cytoplasm after IL-7 treatment (Fig. 6D). The increased abundance of Foxo1 and the decreased abundance of Foxp1 in the nucleus in response to IL-7 were confirmed by Western blotting analysis of fractioned nuclear and cytoplasmic compartments (Fig. 6E). These data suggest that IL-7 signaling increased the nuclear accumulation of Foxo1 and enhanced the translocation of Foxp1 from the nucleus into the cytoplasm, leading to increased Foxo1 binding to the *Il9* promoter by competing with Foxp1.

To further confirm whether Foxo1 and Foxp1 were involved in the enhanced differentiation of IL-7–T_H9 cells, we pretreated Foxo1- and Foxp1-knockout CD4⁺ T cells with IL-7 and then cultured them under T_H9-polarizing conditions. Loss of Foxo1 almost completely abrogated the enhanced differentiation of IL-7–T_H9 cells (Fig. 6, F and G), whereas loss of Foxp1 deficiency promoted their differentiation (Fig. 6, H and I). Because the Foxo family members are characterized by functional redundancy, we used a Foxo1 inhibitor, which can also inhibit Foxo3 and Foxo4 to some degree, to address the relative importance of the Foxo proteins in T_H9 and IL-7–T_H9 cell differentiation. Our results suggest that Foxo inhibition substantially decreased the differentiation of both T_H9 and IL-7–T_H9 cells (Fig. 6, J and K).

Because we showed that IL-7 increased the binding of Foxo1 but decreased the binding of Foxp1 to the *Il9* promoter in naïve CD4⁺ T cells, we wondered whether Foxo1 and Foxp1 could still regulate *Il9* expression during T_H9 cell differentiation. We found that the extent of binding of Foxo1 to the *Il9* promoter was substantially increased in IL-7–T_H9 cells compared to that in T_H9 cells (fig. S8B), which was consistent with the amount of IL-9 produced by these cells (Fig. 1A). T_H9 and IL-7–T_H9 cells did not differ in how much Foxp1 was bound to the *Il9* promoter (fig. S8B). Foxo1 behaved similarly in its binding to the *Il21* promoter as it did to the *Il9* promoter, but Foxp1 did not inhibit *Il21* transcription (Fig. 1D) in IL-7–T_H9 cells, which was evident by the loss of binding of Foxp1 to the *Il21* promoter in IL-7–T_H9 cells (fig. S8C) and was consistent with the time course of *Il21*

expression (Fig. 1D). As expected, Foxo4 behaved similarly to Foxo1 (figs. S7, G and H, and S8).

Because IL-7-mediated enhancement of T_H9 cell differentiation was tightly related with Foxo1 and Foxp1, we hypothesized that the enhanced antitumor activity of these T cells might also be Foxo1-dependent, whereas Foxp1 might inhibit the antitumor activity. Using the therapeutic mouse model, we found that Foxo1 knockout T_H9 cells had compromised antitumor activity compared to WT T_H9 cells (Fig. 6L). Furthermore, loss of Foxo1 also reduced the enhanced antitumor activity of IL-7-T_H9 cells. Conversely, Foxp1 deficiency not only enhanced the antitumor activity of T_H9 cells but also further increased the antitumor activity of the IL-7-T_H9 cells (Fig. 6N). Furthermore, the antitumor activity of T_H9 and IL-7-T_H9 cells seemed to correlate with the number of tumor-infiltrating host CD8⁺ T cells in the mice (Fig. 6, M and O).

DISCUSSION

Although T_H9 cells are considered to be a distinct T_H subset, the transcriptional regulation of IL-9 production and T_H9 cell differentiation remains poorly elucidated. Here, we demonstrate that IL-7-pretreated (programmed) CD4⁺ T cells exhibited enhanced T_H9 cell differentiation potential. Mechanistic studies revealed that IL-7-stimulated STAT5 signaling increased the abundance of the acetyltransferase p300 in a direct transcriptional manner. In addition, IL-7-stimulated STAT5 and PI3K-AKT-mTOR signaling were necessary for the differentiation of both T_H9 and IL-7-T_H9 cells by promoting histone acetylation at the *Il9* promoter. At the same time, p300 acted as a coactivator to enable Foxo1 to bind to the *Il9* promoter to compete with Foxp1. Foxo1 played a positive role in *Il9* transcription, whereas Foxp1 inhibited *Il9* transcription, indicating that Foxp1 may serve as a negative regulator of *Il9* expression in T_H9 cells. The enhanced differentiation and antitumor activity of IL-7-T_H9 cells were Foxo1-dependent, suggesting that Foxo1 is critical in T_H9 cell differentiation and, consequently, in the antitumor activity of these cells.

T_H9 cell differentiation is regulated by multiple transcriptional factors under different situations (29). IL-9 is the hallmark cytokine of T_H9 cells, but *Il9* transcription is temporary and short, so a negative regulatory mechanism that tightly controls *Il9* transcription must exist. One of the factors that inhibit *Il9* transcription is Bcl-6; *Bcl6* expression can be induced by IL-21 but is suppressed by IL-2 (12, 30). However, there is no evidence that Bcl-6 inhibits *Il21* expression, which IL-7-T_H9 cells coexpressed with *Il9*. A study showed that IL-7 inhibits *Bcl6* gene expression in activated CD4⁺ T cells (31), which is consistent with our finding that IL-7 inhibited *Bcl6* transcription in naïve CD4⁺ T cells (fig. S4A). Foxp1 directly binds to the *Il21* promoter during T_{FH} cell differentiation (26), which we also confirmed here. Our results showed that Foxp1 directly repressed *Il9* transcription and that the abundance of Foxp1 protein was increased in differentiating T_H9 cells. Together, our findings suggest that Foxp1 may be a negative regulator of *Il9* expression in T_H9 cells.

IL-7 could temporarily cause bound Foxp1 to dissociate from the *Il9* promoter and translocate from the nucleus into the cytoplasm. However, this cannot be the main mechanism for the enhanced T_H9 cell differentiation that is induced by IL-7 pretreatment.

We demonstrated the existence and role of Foxo1, a positive regulator of *Il9* expression, during the differentiation of T_H9 and IL-7-T_H9 cells. Because Foxp1 and Foxo1 share the same conserved binding sequence on the *Il9* promoter and play a reciprocal role in *Il9* transcription, whichever one of them binds to the *Il9* promoter site must be tightly regulated, probably through competition based on the relative amounts of these proteins or their modifications. IL-7 did not cause any change in Foxo1 mRNA abundance but increased the total amount of Foxo1 protein and decreased the amount of pFoxo1 in IL-7-treated CD4⁺ T cells, leading to the accumulation of more Foxo1 protein in the nucleus and its binding to the *Il9* promoter, which further resulted in increased IL-9 production and enhanced T_H9 cell differentiation. Thus, this study identifies Foxo1 as a positive regulator of *Il9* transcription and IL-9 production in T_H9 cells.

Histone acetylation is important for activating gene expression. For example, histone acetyltransferases, such as GCN5 and p300, positively regulate *Il9* expression, whereas the histone deacetylase SIRT1 inhibits the differentiation of T_H9 cells (32–34). A direct link between IL-7 signaling and increased histone modification has been reported for the TRG locus, and the increased histone acetylation favors the accessibility of Rag enzymes (24). Here, we found that IL-7 enhanced the production of p300 and histone acetylation in a STAT5- and PI3K-AKT-mTOR-dependent manner. It is well known that Foxo1 is activated by p300 through a direct interaction and that p300 also stabilizes Foxo1 protein and increases the amount of Foxo1 protein in the nucleus (35, 36). Although it was reported that IL-7 signaling activates the PI3K-AKT pathway, leading to Foxo1 phosphorylation and its translocation from the nucleus to cytoplasm (23), our studies showed that IL-7 reduced the phosphorylation of Foxo1 and increased its nuclear accumulation, which may be caused by the increased amount of p300. Thus, the increase in both the amount and activity of Foxo1 facilitated its binding to the *Il9* promoter by competing with Foxp1, which was exported to the cytoplasm, to initiate *Il9* transcription. Because T cells also express other Foxo family members, such as Foxo3 and Foxo4, and because the functions of these proteins in T cells are redundant (37), Foxo3 and Foxo4 may also have roles in T_H9 cell differentiation. For this reason, we examined the role of Foxo4 and demonstrated that Foxo4 also enhanced T_H9 cell differentiation. This finding may explain why T_H9 cell differentiation could still be observed, albeit to a lesser extent, in Foxo1-deficient CD4⁺ T cells.

Forkhead box transcription factors are important in the differentiation of T_H cells, including T_{reg} cells, T_H1 cells, and T_{FH} cells, and the maintenance of T cell quiescence. Among the Forkhead box family members, Foxo1 and Foxp1 are the molecules most relevant to IL-7 signaling. The Foxo proteins are the major factors downstream of the IL-7-PI3K-AKT signaling pathway. In T cells, IL-7 signaling activates PI3K and AKT, which phosphorylate Foxo1, and pFoxo1 is exported from the nucleus to the cytoplasm to terminate its transcriptional activity. In B cells, however, the IL-7R-PI3K-AKT pathway regulates the activities of Foxo family proteins in an IL-7 concentration-dependent manner (38). These results may indicate that Foxo1 activity is tightly controlled by different mechanisms. Among those, p300 is one of the most important cofactors for Foxo1. Studies have shown that under different conditions, Foxo1 may exhibit totally opposing activities because of differences in its interaction with p300 (35). Foxo1 and Foxp1 are critical negative regulators of the differentiation of T_{FH} cells (26, 39), and Foxo1 is also involved in the negative

regulation of T_H1 and T_H17 cell differentiation and the positive regulation of T_{reg} cell differentiation (40, 41). Our study demonstrates that Foxo1 and Foxp1 are important positive and negative regulators of T_H9 cell differentiation and activity.

The production of IL-9 and IL-21 is important for the antitumor functions of T_H9 cells (10, 11). We found that IL-7-T_H9 cells produced more IL-21 than did T_H9 cells. In mouse tumor models, IL-21 is important for the survival and proliferation of cytotoxic CD8⁺ T cells and natural killer cells (20, 42). Clinical trials using IL-21 or IL-21 combined with chemotherapy or biological agents are ongoing to treat different tumor types and exhibit great therapeutic potential (43). Compared with the systemic administration of cytokines, the advantage of cellular therapy includes the secretion of multiple cytokines and the potential infiltration of the tumor bed by T cells and their cytokines to exert anti-tumor effects. We suggest that IL-7-T_H9 cells displayed enhanced anti-tumor activity by secreting large amounts of not only IL-9 but also IL-21 and that they could present an effective approach for the development of improved immunotherapeutics.

MATERIALS AND METHODS

Reagents

The Foxo1 inhibitor AS1842856 and the mTOR activator MHY1485 were purchased from Calbiochem; rapamycin and the p300 inhibitor C646 were purchased from Sigma.

Mice and cell lines

C57BL/6 mice were purchased from the National Cancer Institute, and OT-II (C57BL/6-Tg[Tcr α Tcr β]425Cbn/J), Foxo1^{F/F}, Foxo4^{F/F}, CD4Cre, CD4CreERT2, and *Il21r*^{-/-} mice were purchased from The Jackson Laboratory. Foxp1^{F/F} mice were a gift from H. Hu (Department of Microbiology, University of Alabama at Birmingham). Six- to 8-week-old mice were used at the beginning of each experiment. B16-OVA melanoma cell lines were cultured in Iscove's modified Dulbecco's medium (Thermo Fisher Scientific) supplemented with 10% heat-inactivated fetal bovine serum (Thermo Fisher Scientific), penicillin-streptomycin (100 U/ml), and 2 mM L-glutamine (both from Invitrogen). All experiments complied with protocols approved by the Institutional Animal Care and Use Committee at the Cleveland Clinic.

In vitro differentiation of T_H1 and T_H9 cells

Naïve T cells purified from the spleens and lymph nodes of WT or Foxo1 and Foxp1 knockout OT-II mice by FACS (fluorescence-activated cell sorting) sorting or kit (STEMCELL Technologies) were differentiated into T_H1 or T_H9 cells with plate-bound anti-CD3 (2 µg/ml) and soluble anti-CD28 (1 µg/ml) antibodies together with different cytokine combinations: For T_H1 cells, IL-2 (30 ng/ml; R&D Systems), IL-12 (4 ng/ml; R&D Systems), and anti-IL-4 mAb (10 µg/ml; eBioscience) were added; for T_H9 cells, IL-4 (10 ng/ml; R&D Systems), TGF- β (1 ng/ml; R&D Systems), and anti-IFN- γ mAb (10 µg/ml; eBioscience) were added. After 3 days of culture, the differentiated T_H cells were collected, washed, and allowed to continue to differentiate in the presence of the appropriate cytokines.

for 1 day. For IL-7 treatment, naïve T cells were cultured with IL-7 (PeproTech) for 2 days and then washed twice before being differentiated under T_H9-polarizing conditions.

Human CD4⁺ T cell purification and differentiation

Naïve CD4⁺ T cells were isolated from peripheral blood mononuclear cells by negative selection with a kit (Miltenyi Biotec) and stimulated with human T-activator CD3/CD28 Dynabeads (Invitrogen) together with human IL-4 (10 ng/ml), human TGF- β 1 (1 ng/ml), and anti-IFN- γ (10 μ g/ml) for 5 days. Cells were restimulated with PMA and ionomycin for 4 hours with brefeldin A for intracellular staining of IL-9 with PE (phycoerythrin)-conjugated anti-human IL-9 antibody (MH9A4, BioLegend).

Induction of B16 lung melanoma

As was described previously (10), mice were injected intravenously with 2×10^5 B16-OVA cells. For adoptive transfer experiments, mice were injected intravenously with 2×10^6 OVA-specific T_H1, T_H9, or IL-7-T_H9 cells on the same day in the prophylactic model or 4 days after tumor injection in the therapeutic model. At day 14 or 15 after tumor injection, mice were sacrificed for enumeration of metastatic lung foci. All lung lobes were evaluated under a tissue dissect microscope. For some experiments, anti-IL-9 and anti-IL-21R (both from Bio X Cell) and IL-7 antibodies were used as indicated.

Gene microarrays

Total RNA was extracted with TRIzol reagent from naïve CD4⁺ T cells that had been treated with or without IL-7 or from differentiated T_H9 or IL-7-T_H9 cells. The microarray was performed with the MouseRef-8 v2.0 Expression BeadChip Kit in the Cleveland Clinic Genomic Core.

Western blotting

Cells were washed with PBS twice and then lysed in 1 \times lysis buffer (Cell Signaling) with protease cocktail (Roche), which was followed by sonication. Cell lysates were resolved by SDS-polyacrylamide gel electrophoresis gel (Fisher) and then analyzed by Western blotting with the appropriate antibodies (all from Cell Signaling). For the fractionation of cells into nuclear and cytoplasmic fractions, the Cell Fractionation Kit (Cell Signaling) was used according to the manufacturer's protocol.

Viral transduction

Complementary DNAs (cDNAs) encoding Foxo1 and Foxo4 were synthesized and subcloned into the MigR1 retroviral vector. Foxp1-specific shRNA (GCCCATTTTCGTCAGCAGATAT) was synthesized by Sigma and subcloned into the pLKO.1-GFP lentiviral vector. Viruses were packaged in 293T cells transfected with Lipofectamine 2000 (Life Sciences). Virus-containing cell culture medium was harvested from the cells on days 1 to 3, filtered through a 0.45- μ m filter, concentrated with PEG-it Virus Precipitation Solution, and stored at -80°C until use. Naïve or activated CD4⁺ T cells were mixed with virus and protamine sulfate (10 μ g/ml; Sigma) in a 24-well plate, followed by centrifugation for 120 min at 500g at 32°C. After 2 hours of incubation, the activated

CD4⁺ T cells were differentiated, as described earlier. Three days later, GFP⁺ cells were sorted by FACS for Western blotting analysis to check the efficiency of overexpression or knockdown efficiency (fig. S9). Total cells were harvested and analyzed by flow cytometry.

Flow cytometry

Polarized T_H cells were stimulated with PMA (50 ng/ml; Sigma-Aldrich) and ionomycin (500 ng/ml; Sigma-Aldrich) and blocked by brefeldin A (BioLegend) for 4 hours. Cells were first stained with anti-CD4 antibody and then fixed and stained with the BD Cell Fixation/Permeabilization Kit (for cytokines) or the Foxp3/Transcription Factor Staining Kit (for Foxp3). Cells were analyzed with BD Calibur, BD Fortessa, or Miltenyi MACSQuant systems. Data were analyzed with FlowJo software (TreeStar). The mAbs used for flow cytometry were as follows: FITC-conjugated anti-CD4 (GK1.5, BD Biosciences) and PE-conjugated anti-IL-9 (D9302C12, BD Biosciences), IL-21R-Fc chimera (991-R2-100, R&D Systems), and Alexa Fluor 647-conjugated affinity-purified goat antibody [F(ab)₂ fragment] specific for the Fcγ fragment of human IgG (109-606-008, Jackson ImmunoResearch Laboratories).

Measurement of cytokines

Cells were harvested, counted, and restimulated with anti-CD3 or with PMA and ionomycin for 12 hours. Cell culture medium was collected and analyzed by ELISA to determine the concentrations of mouse IL-9 and IL-21 (all from R&D Systems) according to the manufacturer's protocol.

ChIP assay

SimpleChIP Plus Enzymatic Chromatin IP Kits were used for ChIP assay according to the manufacturer's protocol, and DNAs were measured by real-time quantitative PCR. Antibodies used for ChIP assay were against the following targets: IRF4, PU.1, Foxo1, Foxo4, and Foxp1 (all from Cell Signaling). Primers designed for the ChIP assay are as follows: *Il9* promoter negative control (forward, 5'-GCCTGCAAGTTT-CTGGACAA-3'; reverse, 5'-GAATATGGGTGGGAGTGGGT-3'); CNS on the *Il9* promoter (forward, 5'-AAAGATCTAGCCCCAACCCC-3'; reverse, 5'-TGACCCCTTCATTACCACCC-3'); *Il21* promoter control region (forward, 5'-GCAGTAAGGGAAGAAGGTCAAG-3'; reverse, 5'-GGGCTGGATTGTGGAAAGA-3'); and *p300* promoter region (forward, 5'-AGGGATGGATAGAGTCCACAA-3'; reverse, 5'-GCTGCTTTACTCATTGCAGAAG-3').

Luciferase transactivation assay

Mouse *Il9* (from -895 to +5) and *Il21* promoters were synthesized and subcloned into the pGL3 basic vector (Promega). 293T cells were transiently transfected for 24 hours with reporter plasmids, Renilla (for internal normalization), and the plasmid pcDNA3.1-Foxo1, pcDNA3.1-Foxp1, or pcDNA3.1-p300 (all from Addgene and subcloned into the pcDNA3.1 plasmid) with Lipofectamine 2000 (Invitrogen). EL4 cells were transfected with p300 reporter and pcDNA3.1-STAT5 plasmids by the Lonza Nucleofector 2b Device. Luciferase was measured with the Dual-Luciferase Reporter Assay System (Promega) according to the manufacturer's instructions.

Real-time quantitative PCR

Total RNA from T cells was extracted with TRIzol, and cDNA was synthesized with M-MLV reverse transcriptase (Invitrogen) and analyzed by real-time quantitative PCR by SYBR Green (Applied Biosystems). The abundances of the mRNAs of interest were normalized to that of the mouse housekeeping gene *actb*. The primers used were as follows: *Il9* (forward, 5'-CTGATGATTGTACCACACCGTGC-3'; reverse, 5'-GCCTTTGCATCTCTGTCTTCTGG-3'); *Il21* (forward, 5'-AAGATT-CCTGAGGATCCGAGAAG-3'; reverse, 5'-GCATTCGTGAGCGTCTA-TAGTGTC-3'); *Foxo1* (forward, 5'-CCGGAGTTTAACCAGTCCAA-3'; reverse, 5'-TGCTCATAAAGTCGGTGCTG-3'); *Foxp1* (forward, 5'-CTGAATCTGGTATCAAGTGTACCCCTCT-3'; reverse, 5'-GATTCGA-GAATGGCCTGCCTGA-3'); *Foxo4* (forward, 5'-TGACCAGTGCAGGT-TAGTGC-3'; reverse, 5'-CTGCTACACAGCCTTCCACA-3'); *p300* (forward, 5'-TCACCTCCTAGCCGAGAAGA-3'; reverse, 5'-ACGGATCA-TAGACGGGTCAG-3'); *GCN5* (forward, 5'-ACTGGTGCCTGAGAAGAG-GA-3'; reverse, 5'-CTCCCATGGAAGGACTGAAG-3'); *PCAF* (forward, 5'-AGTGCCATGGTTCCTTGTTC-3'; reverse, 5'-CCAAGTGAGAAACGT-GAGCA-3'); *Bcl6* (forward, 5'-CACACCCGTCCATCATTGAA-3'; reverse, 5'-TGTCCTCACGGTGCCTTTTT-3'); *IRF4* (forward, 5'-ACG-CTGCCCTCTTCAAGGCTT-3'; reverse, 5'-TGGCTCCTCTCGACC-AATTCC-3'); *PU.1* (forward, 5'-GGAGAAGCTGATGGCTTGG-3'; reverse, 5'-CAGGCGAATCTTTTCTTGC-3'); *Tbx21* (forward, 5'-CAACA-ACCCCTTTGCCAAAG-3'; reverse, 5'-TCCCCCAAGCAGTTGACAGT-3'); *Foxp3* (forward, 5'-CTCGTCTGAAGGCAGAGTCA-3'; reverse, 5'-TG-GCAGAGAGGTATTGAGGG-3'); *Gata3* (forward, 5'-AGGGACA-TCCTGCGCGAACTGT-3'; reverse, 5'-CATCTTCCGGTTTCGGGTCTGG-3'); *c-maf* (forward, 5'-AGCAGTTGGTGACCATGTGCG-3'; reverse, 5'-TGGA-GATCTCCTGCTTGAGG-3'); *Batf* (forward, 5'-GTTCTG-TTTCTCCAGGTCC-3'; reverse, 5'-GAAGAATCGCATCGCTGC-3'); *ROR γ t* (forward, 5'-TGAGGCCATTAGTATGTGG-3'; reverse, 5'-CTTC-CATTGCTCCTGCTTTC-3'); *Nfatc1* (forward, 5'-CTTCCAGC-CTGTCTTCTTGG-3'; reverse, 5'-TGCAAACACAAGCTCTGTCC-3'); and *actb* (forward, 5'-TGGAATCCTGTGGCATCCATGAAAC-3'; reverse, 5'-TAAACGCAGCTCAGTAACAGTCCG-3').

Immunofluorescence microscopy

Naïve CD4⁺ T cells that were untreated or treated with IL-7 for 2 days were centrifuged onto glass coverslips, and the cells were then washed with PBS, fixed for 5 min in cold methanol, and permeabilized in 75% ethanol. After rehydration with PBS at 25°C, the coverslips were blocked and stained with primary antibodies for Foxo1 or Foxp1, followed by incubation with rhodamine-labeled secondary antibody and DAPI. Images were acquired with a Leica TCS-SP5II upright confocal microscope (Leica Microsystems).

Statistical analysis

A two-tailed Student's *t* test was used for statistical analyses. $P < 0.05$ was considered to be statistically significant. Results are presented as means \pm SD.

Supplementary Material

Refer to Web version on PubMed Central for supplementary material.

Acknowledgments

We thank H. Hu (Department of Microbiology, University of Alabama at Birmingham) for providing the Foxp1^{F/F} mice. We thank C. Talerico, a salaried employee of the Cleveland Clinic, for substantive editing and comments.

Funding: This work was supported by grants from the National Cancer Institute (R01 CA163881, R01 CA200539, R01 CA211073, and K99 CA190910), 4R00CA190910-03, the Leukemia and Lymphoma Society (6469-15), and the Multiple Myeloma Research Foundation.

REFERENCES AND NOTES

1. Zhu J, Yamane H, Paul WE. Differentiation of effector CD4 T cell populations. *Annu Rev Immunol*. 2010; 28:445–489. [PubMed: 20192806]
2. Gessner A, Blum H, Rölinghoff M. Differential regulation of IL-9-expression after infection with *Leishmania major* in susceptible and resistant mice. *Immunobiology*. 1993; 189:419–435. [PubMed: 8125519]
3. Schmitt E, Germann T, Goedert S, Hoehn P, Huels C, Koelsch S, Kühn R, Müller W, Palm N, Rüde E. IL-9 production of naive CD4+ T cells depends on IL-2, is synergistically enhanced by a combination of TGF-beta and IL-4, and is inhibited by IFN-gamma. *J Immunol*. 1994; 153:3989–3996. [PubMed: 7930607]
4. Dardalhon V, Awasthi A, Kwon H, Galileos G, Gao W, Sobel RA, Mitsdoerffer M, Strom TB, Elyaman W, Ho I-C, Khoury S, Oukka M, Kuchroo VK. IL-4 inhibits TGF- β -induced Foxp3⁺ T cells and, together with TGF- β , generates IL-9⁺ IL-10⁺ Foxp3⁺ effector T cells. *Nat Immunol*. 2008; 9:1347–1355. [PubMed: 18997793]
5. Chang HC, Sehra S, Goswami R, Yao W, Yu Q, Stritesky GL, Jabeen R, McKinley C, Ahyi AN, Han L, Nguyen ET, Robertson MJ, Perumal NB, Tepper RS, Nutt SL, Kaplan MH. The transcription factor PU.1 is required for the development of IL-9-producing T cells and allergic inflammation. *Nat Immunol*. 2010; 11:527–534. [PubMed: 20431622]
6. Veldhoen M, Uytendhoeve C, van Snick J, Helmby H, Westendorf A, Buer J, Martin B, Wilhelm C, Stockinger B. Transforming growth factor- β 'reprograms' the differentiation of T helper 2 cells and promotes an interleukin 9-producing subset. *Nat Immunol*. 2008; 9:1341–1346. [PubMed: 18931678]
7. Yao W, Zhang Y, Jabeen R, Nguyen ET, Wilkes DS, Tepper RS, Kaplan MH, Zhou B. Interleukin-9 is required for allergic airway inflammation mediated by the cytokine TSLP. *Immunity*. 2013; 38:360–372. [PubMed: 23376058]
8. Faulkner H, Humphreys N, Renaud JC, van Snick J, Grencis R. Interleukin-9 is involved in host protective immunity to intestinal nematode infection. *Eur J Immunol*. 1997; 27:2536–2540. [PubMed: 9368607]
9. Purwar R, Schlapbach C, Xiao S, Kang HS, Elyaman W, Jiang X, Jetten AM, Khoury SJ, Fuhlbrigge RC, Kuchroo VK, Clark RA, Kupper TS. Robust tumor immunity to melanoma mediated by interleukin-9-producing T cells. *Nat Med*. 2012; 18:1248–1253. [PubMed: 22772464]
10. Lu Y, Hong S, Li H, Park J, Hong B, Wang L, Zheng Y, Liu Z, Xu J, He J, Yang J, Qian J, Yi Q. Th9 cells promote antitumor immune responses in vivo. *J Clin Invest*. 2012; 122:4160–4171. [PubMed: 23064366]
11. Végran F, Berger H, Boidot R, Mignot G, Bruchard M, Dosset M, Chalmin F, Rébé C, Dérangère V, Ryffel B, Kato M, Prévost-Blondel A, Ghiringhelli F, Apetoh L. The transcription factor IRF1

- dictates the IL-21-dependent anticancer functions of T_H9 cells. *Nat Immunol.* 2014; 15:758–766. [PubMed: 24973819]
12. Liao W, Spolski R, Li P, Du N, West EE, Ren M, Mitra S, Leonard WJ. Opposing actions of IL-2 and IL-21 on Th9 differentiation correlate with their differential regulation of BCL6 expression. *Proc Natl Acad Sci U S A.* 2014; 111:3508–3513. [PubMed: 24550509]
 13. Takada K, Jameson SC. Naive T cell homeostasis: From awareness of space to a sense of place. *Nat Rev Immunol.* 2009; 9:823–832. [PubMed: 19935802]
 14. Boerman OC, Gregorio TA, Grzegorzewski KJ, Faltynek CR, Kenny JJ, Wiltout RH, Komschlies KL. Recombinant human IL-7 administration in mice affects colony-forming units-spleen and lymphoid precursor cell localization and accelerates engraftment of bone marrow transplants. *J Leukoc Biol.* 1995; 58:151–158. [PubMed: 7643010]
 15. Chung B, Dudl E, Toyama A, Barsky L, Weinberg KI. Importance of interleukin-7 in the development of experimental graft-versus-host disease. *Biol Blood Marrow Transplant.* 2008; 14:16–27.
 16. Morrissey PJ, Conlon P, Braddy S, Williams DE, Namen AE, Mochizuki DY. Administration of IL-7 to mice with cyclophosphamide-induced lymphopenia accelerates lymphocyte repopulation. *J Immunol.* 1991; 146:1547–1552. [PubMed: 1993845]
 17. Tang J-C, Shen G-B, Wang S-M, Wan Y-S, Wei Y-Q. IL-7 inhibits tumor growth by promoting T cell-mediated antitumor immunity in Meth A model. *Immunol Lett.* 2014; 158:159–166. [PubMed: 24406503]
 18. Pellegrini M, Mak TW. Tumor immune therapy: Lessons from infection and implications for cancer—Can IL-7 help overcome immune inhibitory networks? *Eur J Immunol.* 2010; 40:1852–1861. [PubMed: 20518034]
 19. Colombetti S, Lévy F, Chapatte L. IL-7 adjuvant treatment enhances long-term tumor-antigen-specific CD8⁺ T-cell responses after immunization with recombinant lentivector. *Blood.* 2009; 113:6629–6637. [PubMed: 19383968]
 20. Liu S, Lizée G, Lou Y, Liu C, Overwijk WW, Wang G, Hwu P. IL-21 synergizes with IL-7 to augment expansion and anti-tumor function of cytotoxic T cells. *Int Immunol.* 2007; 19:1213–1221. [PubMed: 17898044]
 21. Rathmell JC, Farkash EA, Gao W, Thompson CB. IL-7 enhances the survival and maintains the size of naive T cells. *J Immunol.* 2001; 167:6869–6876. [PubMed: 11739504]
 22. Seki, Y-i, Yang, J., Okamoto, M., Tanaka, S., Goitsuka, R., Farrar, MA., Kubo, M. IL-7/STAT5 cytokine signaling pathway is essential but insufficient for maintenance of naive CD4 T cell survival in peripheral lymphoid organs. *J Immunol.* 2007; 178:262–270. [PubMed: 17182563]
 23. Barata JT, Silva A, Brandao JG, Nadler LM, Cardoso AA, Boussiotis VA. Activation of PI3K is indispensable for interleukin 7-mediated viability, proliferation, glucose use, and growth of T cell acute lymphoblastic leukemia cells. *J Exp Med.* 2004; 200:659–669. [PubMed: 15353558]
 24. Huang J, Durum SK, Muegge K. Cutting edge: Histone acetylation and recombination at the TCRg locus follows IL-7 induction. *J Immunol.* 2001; 167:6073–6077. [PubMed: 11714763]
 25. Waickman AT, Powell JD. mTOR, metabolism, and the regulation of T-cell differentiation and function. *Immunol Rev.* 2012; 249:43–58. [PubMed: 22889214]
 26. Wang H, Geng J, Wen X, Bi E, Kossenkova AV, Wolf AI, Tas J, Choi YS, Takata H, Day TJ, Chang LY, Sprout SL, Becker EK, Willen J, Tian L, Wang X, Xiao C, Jiang P, Crotty S, Victora GD, Showe LC, Tucker HO, Erikson J, Hu H. The transcription factor Foxp1 is a critical negative regulator of the differentiation of follicular helper T cells. *Nat Immunol.* 2014; 15:667–675. [PubMed: 24859450]
 27. Ouyang W, Beckett O, Flavell RA, Li MO. An essential role of the Forkhead-box transcription factor Foxo1 in control of T cell homeostasis and tolerance. *Immunity.* 2009; 30:358–371. [PubMed: 19285438]
 28. Feng X, Ippolito GC, Tian L, Wiehagen K, Oh S, Sambandam A, Willen J, Bunte RM, Maika SD, Harriss JV, Caton AJ, Bhandoola A, Tucker PW, Hu H. Foxp1 is an essential transcriptional regulator for the generation of quiescent naive T cells during thymocyte development. *Blood.* 2010; 115:510–518. [PubMed: 19965654]

29. Kaplan MH, Hufford MM, Olson MR. The development and in vivo function of T helper 9 cells. *Nat Rev Immunol.* 2015; 15:295–307. [PubMed: 25848755]
30. Bassil R, Orent W, Olah M, Kurdi AT, Frangieh M, Buttrick T, Khoury SJ, Elyaman W. BCL6 controls Th9 cell development by repressing *Il9* transcription. *J Immunol.* 2014; 193:198–207. [PubMed: 24879792]
31. McDonald PW, Read KA, Baker CE, Anderson AE, Powell MD, Ballesteros-Tato A, Oestreich KJ. IL-7 signalling represses Bcl-6 and the T_{FH} gene program. *Nat Commun.* 2016; 7:10285. [PubMed: 26743592]
32. Goswami R, Kaplan MH. Gcn5 is required for PU.1-dependent IL-9 induction in Th9 cells. *J Immunol.* 2012; 189:3026–3033. [PubMed: 22904310]
33. Xiao X, Shi X, Fan Y, Zhang X, Wu M, Lan P, Minze L, Fu YX, Ghobrial RM, Liu W, Li XC. GITR subverts Foxp3⁺ Tregs to boost Th9 immunity through regulation of histone acetylation. *Nat Commun.* 2015; 6:8266. [PubMed: 26365427]
34. Wang Y, Bi Y, Chen X, Li C, Li Y, Zhang Z, Wang J, Lu Y, Yu Q, Su H, Yang H, Liu G. Histone deacetylase SIRT1 negatively regulates the differentiation of interleukin-9-producing CD4⁺ T cells. *Immunity.* 2016; 44:1337–1349. [PubMed: 27317260]
35. van der Heide LP, Smidt MP. Regulation of FoxO activity by CBP/p300-mediated acetylation. *Trends Biochem Sci.* 2005; 30:81–86. [PubMed: 15691653]
36. Perrot V, Rechler MM. The coactivator p300 directly acetylates the forkhead transcription factor Foxo1 and stimulates Foxo1-induced transcription. *Mol Endocrinol.* 2005; 19:2283–2298. [PubMed: 15890677]
37. Hedrick SM, Michelini R, Hess, Doedens AL, Goldrath AW, Stone EL. FOXO transcription factors throughout T cell biology. *Nat Rev Immunol.* 2012; 12:649–661. [PubMed: 22918467]
38. Ochiai K, Maienschein-Cline M, Mandal M, Triggs JR, Bertolino E, Sciammas R, Dinner AR, Clark MR, Singh H. A self-reinforcing regulatory network triggered by limiting IL-7 activates pre-BCR signaling and differentiation. *Nat Immunol.* 2012; 13:300–307. [PubMed: 22267219]
39. Stone EL, Pepper M, Katayama CD, Kerdiles YM, Lai CY, Emslie E, Lin YC, Yang E, Goldrath AW, Li MO, Cantrell DA, Hedrick SM. ICOS coreceptor signaling inactivates the transcription factor FOXO1 to promote Tfh cell differentiation. *Immunity.* 2015; 42:239–251. [PubMed: 25692700]
40. Lainé A, Martin B, Luka M, Mir L, Auffray C, Lucas B, Bismuth G, Charvet C. Foxo1 is a T cell–intrinsic inhibitor of the ROR γ t-Th17 program. *J Immunol.* 2015; 195:1791–1803. [PubMed: 26170390]
41. Ouyang W, Liao W, Luo CT, Yin N, Huse M, Kim MV, Peng M, Chan P, Ma Q, Mo Y, Meijer D, Zhao K, Rudensky AY, Atwal G, Zhang MQ, Li MO. Novel Foxo1-dependent transcriptional programs control T_{reg} cell function. *Nature.* 2012; 491:554–559. [PubMed: 23135404]
42. Markley JC, Sadelain M. IL-7 and IL-21 are superior to IL-2 and IL-15 in promoting human T cell-mediated rejection of systemic lymphoma in immunodeficient mice. *Blood.* 2010; 115:3508–3519. [PubMed: 20190192]
43. Spolski R, Leonard WJ. Interleukin-21: A double-edged sword with therapeutic potential. *Nat Rev Drug Discov.* 2014; 13:379–395. [PubMed: 24751819]

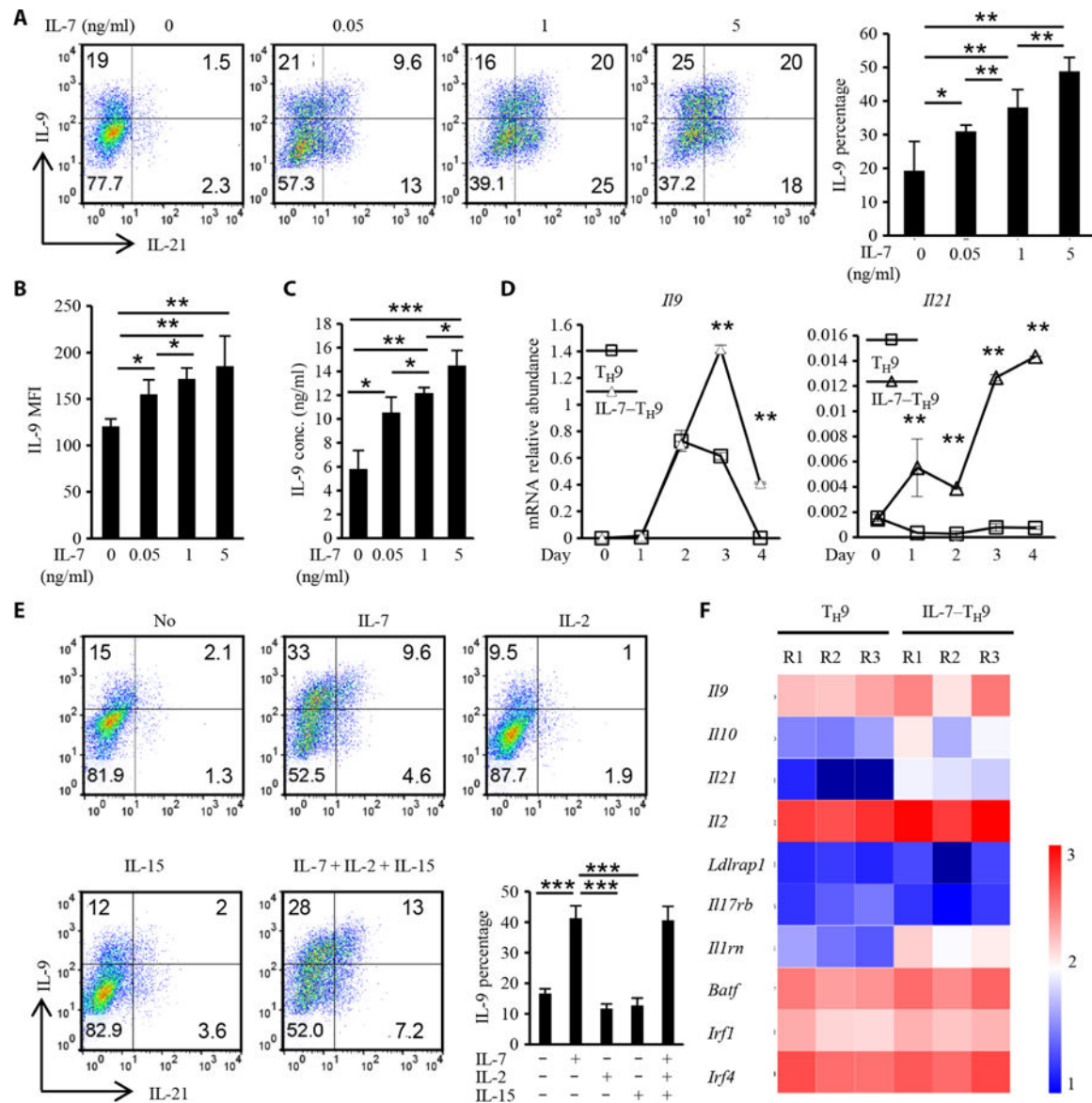


Fig. 1. Pretreatment of naïve CD4⁺ T cells with IL-7 enhances their differentiation into T_H9 cells (A to C) Naïve OT-II CD4⁺ T cells were cultured with the indicated concentrations of IL-7 for 2 days, washed twice with T cell medium, and then cultured for 4 days under the T_H9-polarizing conditions. Freshly isolated naïve CD4⁺ T cells that were not pretreated with IL-7 were used as a control. The cells were then harvested and restimulated with PMA and ionomycin in the presence of brefeldin A for 4 hours. The cells were then analyzed by flow cytometry to detect IL-9 and IL-21 (A, dot plots), to determine the percentages of IL-9-expressing cells (A, bar graph), and to calculate the MFI of IL-9 (B). Alternatively, the cells were stimulated with anti-CD3 (1 µg/ml) for 12 hours, and the cell culture medium was analyzed by ELISA to determine the amount of secreted IL-9 (C). (D) T_H9 cells (open squares) and IL-7-T_H9 cells (open triangles) were harvested on the indicated days of T_H9 cell differentiation, and RNA was extracted and used for real-time PCR analysis of the relative abundances of *Il9* and *Il21* mRNAs, which were normalized to that of mouse *actb*

mRNA. **(E)** Naïve OT-II CD4⁺ T cells were pretreated with the indicated γ C family cytokines for 2 days, washed twice, and then cultured under T_H9-polarizing conditions for 4 days. The cells were then analyzed by flow cytometry to detect IL-9 and IL-21 (dot plots) and to determine the percentages of IL-9-expressing cells (bar graph). **(F)** T_H9 and IL-7–T_H9 cells were collected on day 3, and RNA was extracted for gene microarray analysis. The expression of T_H9 cell–related genes, including those encoding cytokines and transcription factors, is shown. R1 to R3 indicate three replicates. Data in (A) to (E) are means \pm SD of three independent experiments. * P < 0.05, ** P < 0.01, *** P < 0.001.

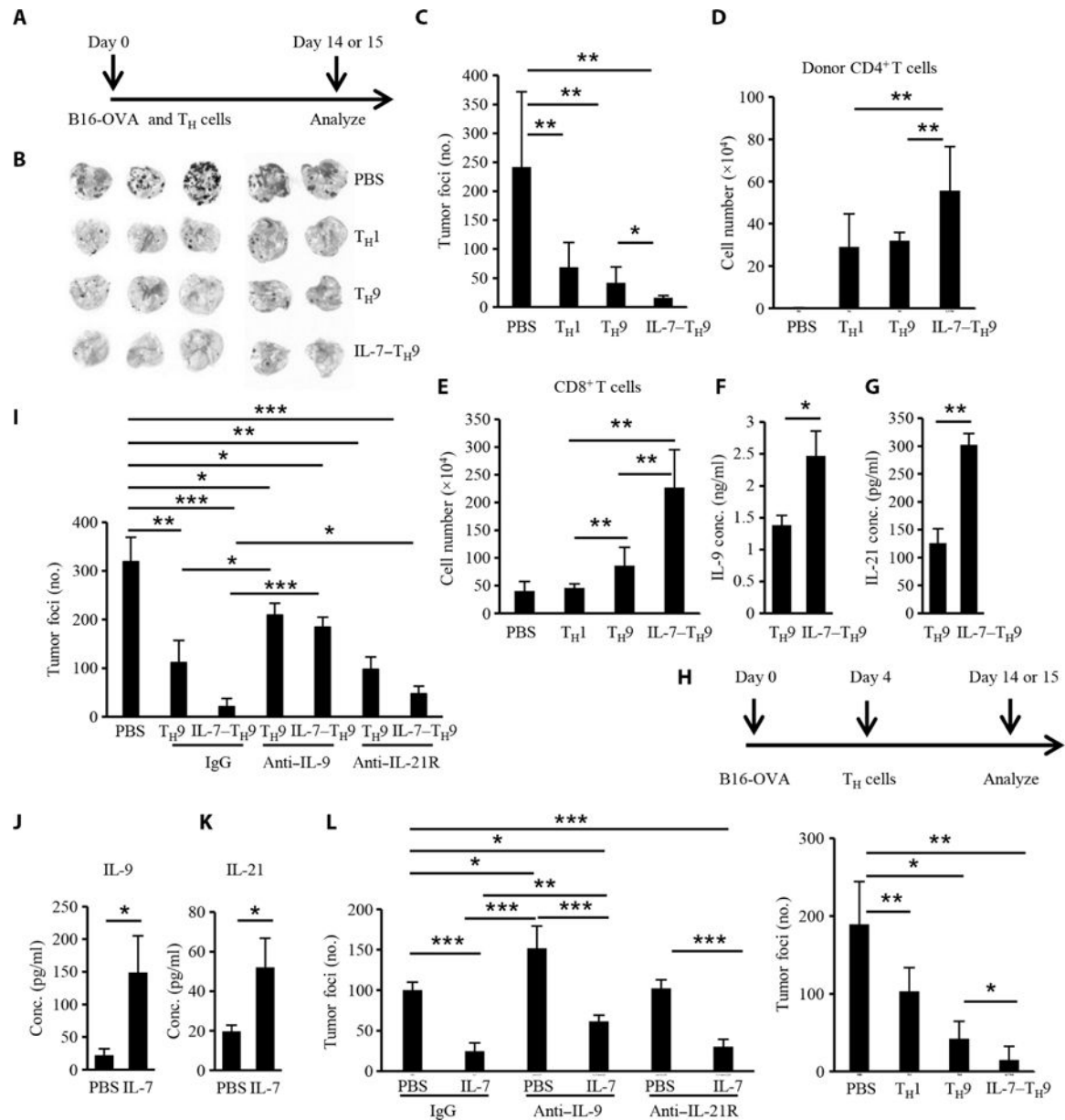


Fig. 2. IL-7-T_H9 cells have enhanced antitumor activity

(A to G) C57BL/6 mice (five mice per group) were challenged with 2×10^5 B16-OVA cells, which was followed by the transfer of 2×10^6 T_H1, T_H9, or IL-7-T_H9 cells from CD45.1 OT-II mice on the same day. On day 14, the mice were sacrificed and tissues were harvested for different assays. (A) Schematic showing the time course of the prophylactic model. (B) Images of lungs showing tumor development and foci in the different treatment groups. PBS, phosphate-buffered saline. (C) Lung tumor foci numbers according to the indicated treatment. (D) Numbers of adoptively transferred CD4⁺ T cells in the lungs of the recipient mice. (E) Numbers of CD8⁺ T cells that infiltrated the lungs for the indicated treatments. (F and G) Donor-derived CD4⁺ T cells from lung lymph nodes in the T_H9 and IL-7-T_H9 groups were sorted and stimulated with PMA and ionomycin. The amounts of IL-9 (F) and IL-21 (G) in the cell culture medium were determined by ELISA. (H) Therapeutic effect of

T_H cells in the B16-OVA lung model. Similarly to the prophylactic model, T cells were transferred to mice (four to five mice per group) on day 4 after tumor injection. (I) Numbers of tumor foci in the lungs according to the treatment group. In the therapeutic model (five mice per group), anti-IL-9 and anti-IL-21R antibodies (both at 200 μ g per mice per injection) were injected intraperitoneally every other day, beginning 1 day before the T_H9 cells were transferred, and tumor foci were analyzed on day 14. IgG, immunoglobulin G. (J to L) C57BL/6 mice (four to five mice per group) were injected with B16 tumor cells and received IL-7 (5 μ g per injection) or PBS daily from the same day for 14 days. Anti-IL-9 or anti-IL-21R antibodies were injected every other day, and 1 day before IL-7 injection in the indicated groups. Then, mice were sacrificed on day 14, lung lymph nodes were collected from the PBS and IL-7 only groups, and total $CD4^+$ T cells were isolated and stimulated with PMA and ionomycin before the amounts of IL-9 (J) and IL-21 (K) released into the cell culture medium were determined by ELISA. (L) The numbers of tumor foci were counted in all groups. Data in (B) to (L) were from three independent experiments and are presented as means \pm SD. * $P < 0.05$, ** $P < 0.01$, *** $P < 0.001$.

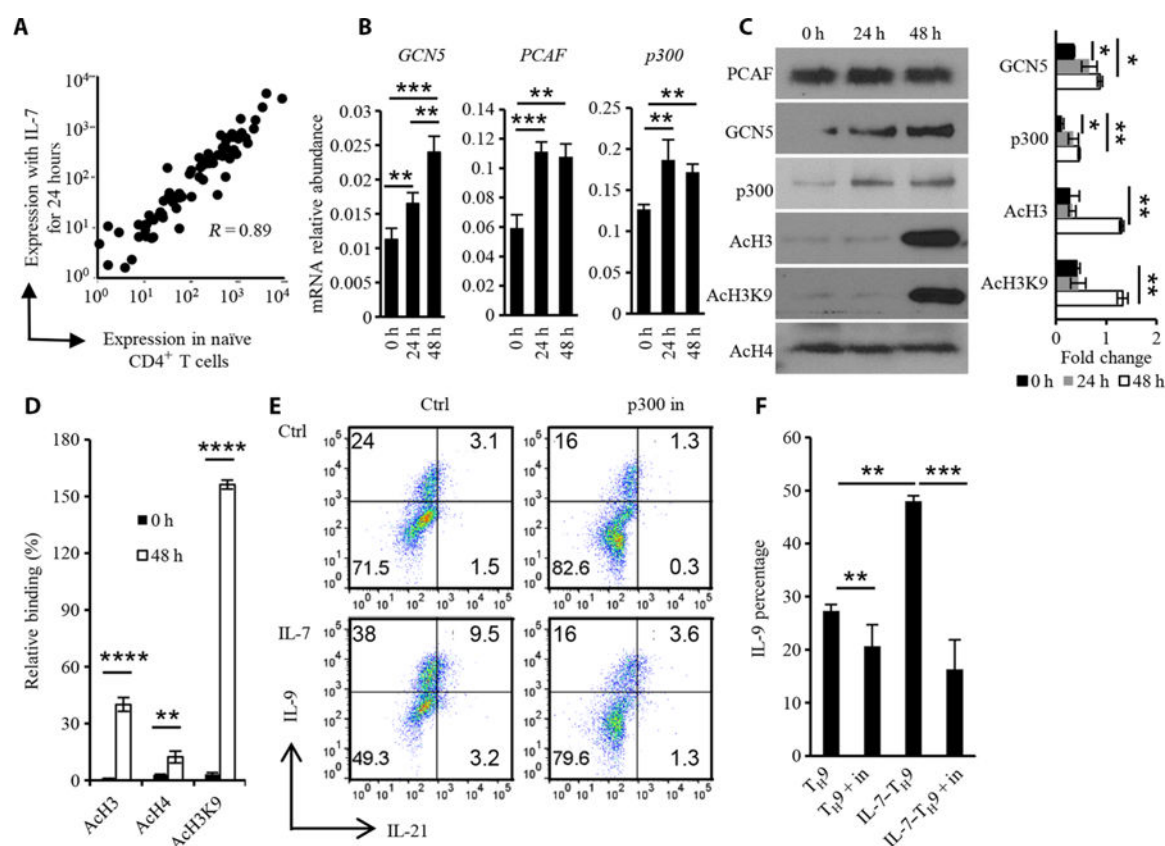


Fig. 3. IL-7 promotes histone acetylation at the *Il9* promoter

(A) Naïve OT-II CD4⁺ T cells were treated with IL-7 (1 ng/ml) for 0 or 24 hours, and RNA was extracted for gene microarray analysis. The expression of genes encoding selected T cell transcriptional factors with or without IL-7 treatment was determined. (B) Real-time PCR analysis was performed to determine the extent of expression of genes encoding the histone acetyltransferases GCN5, PCAF, and p300 in the T cells after IL-7 treatment for 24 or 48 hours. PCR results were normalized to mouse *actb* to show the mRNA relative abundance. (C) Naïve CD4⁺ T cells were treated with IL-7 for the indicated times before being analyzed by Western blotting with antibodies against the indicated proteins. (D) ChIP analysis of acetylated (Ac) H3 (AcH3), H4 (AcH4), and H3K9 (AcH3K9) at the *Il9* promoter region in naïve CD4⁺ T cells that were untreated or were treated with IL-7 for 48 hours. Data were normalized to the control region. (E) Effect of a p300 inhibitor (p300 in) on T_H9 and IL-7-T_H9 cell differentiation. Naïve CD4⁺ T cells were pretreated with IL-7 for 2 days, washed twice, and polarized under T_H9 conditions in the presence or absence of 5 μ M C646 for 4 days. Naïve CD4⁺ T cells polarized under T_H9 conditions without IL-7 pretreatment served as the T_H9 control (Ctrl). Cells positive for IL-9 and IL-21 were determined by flow cytometry. (F) Percentages of IL-9⁺ T cells under the indicated conditions. Data in (C) to (F) are from three independent experiments and are presented as means \pm SD. * $P < 0.05$, ** $P < 0.01$, *** $P < 0.001$, **** $P < 0.0001$.

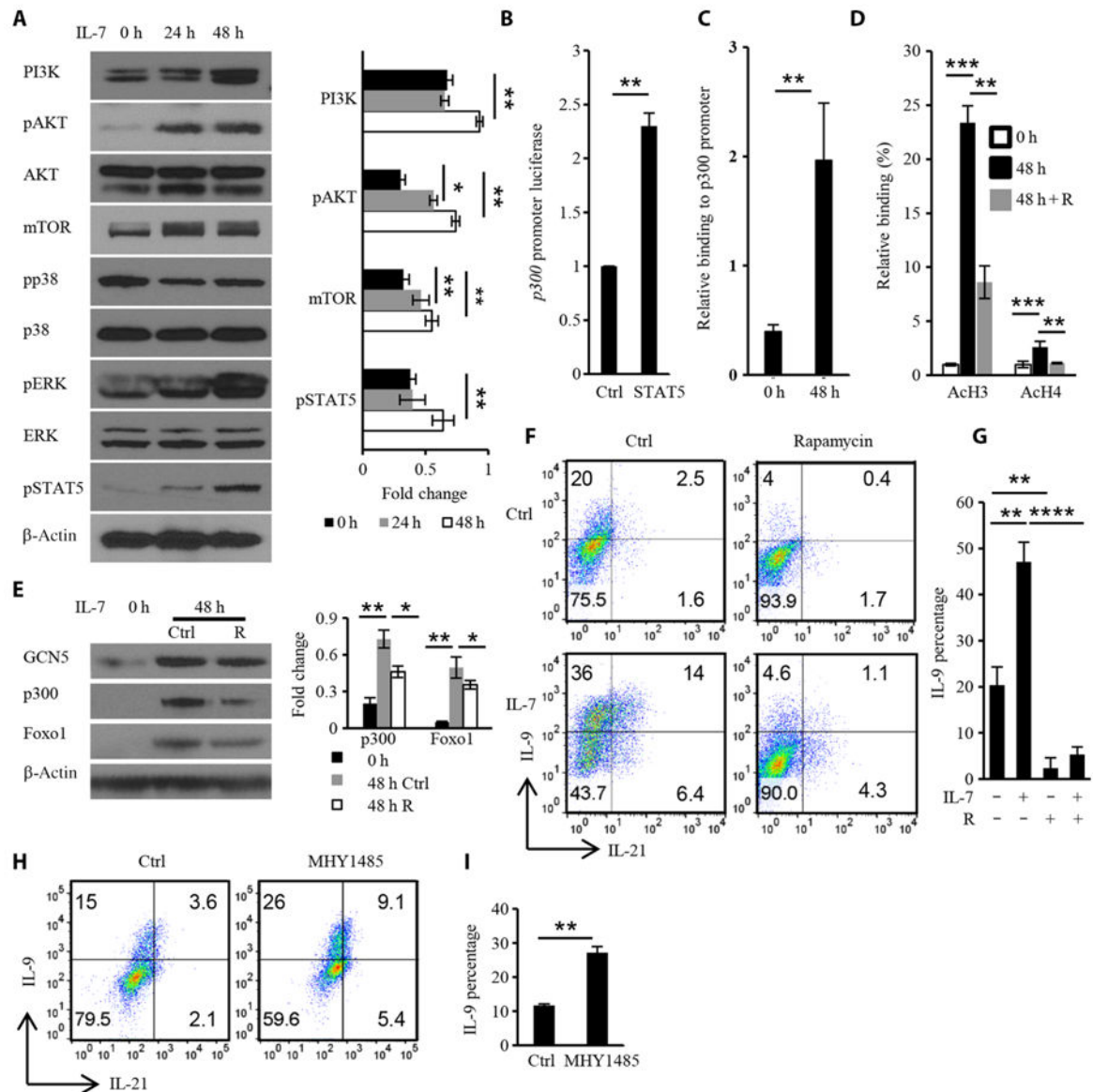


Fig. 4. IL-7 promotes chromatin modification at the *Il9* promoter and T_H9 cell differentiation in a PI3K-AKT-mTOR-dependent manner

(A) Naïve OT-II $CD4^+$ T cells were cultured for the indicated times with IL-7 (1 ng/ml), washed, and analyzed by Western blotting with antibodies against the indicated proteins to demonstrate signaling downstream of IL-7. Right: Densitometric analysis of the indicated band intensities. (B) EL4 cells were transfected with plasmids encoding the p300 promoter with or without the STAT5-expressing plasmid pcDNA3.1. Forty-eight hours later, the luciferase activity of the p300 promoter reporter was detected and normalized to that of *Renilla* luciferase. (C) ChIP analysis of the effect of IL-7 on the binding of STAT5 to the p300 promoter. (D) ChIP analysis of the inhibitory effect of rapamycin (R) on IL-7-induced histone acetylation after 48 hours of treatment. (E) Naïve OT-II $CD4^+$ T cells were treated with IL-7 alone or in the presence of rapamycin for 48 hours before being analyzed by Western blotting with antibodies against the indicated proteins. (F to I) Naïve OT-II $CD4^+$ T

cells or IL-7-pretreated OT-II CD4⁺ T cells were cultured under T_H9 conditions in the presence or absence of 30 nM rapamycin (F and G) or 1 μM MHY1485 (H and I) and then were analyzed by flow cytometry to detect IL-9 and IL-21. Data are from three independent experiments and are means ± SD. **P* < 0.05, ***P* < 0.01, ****P* < 0.001, *****P* < 0.0001.

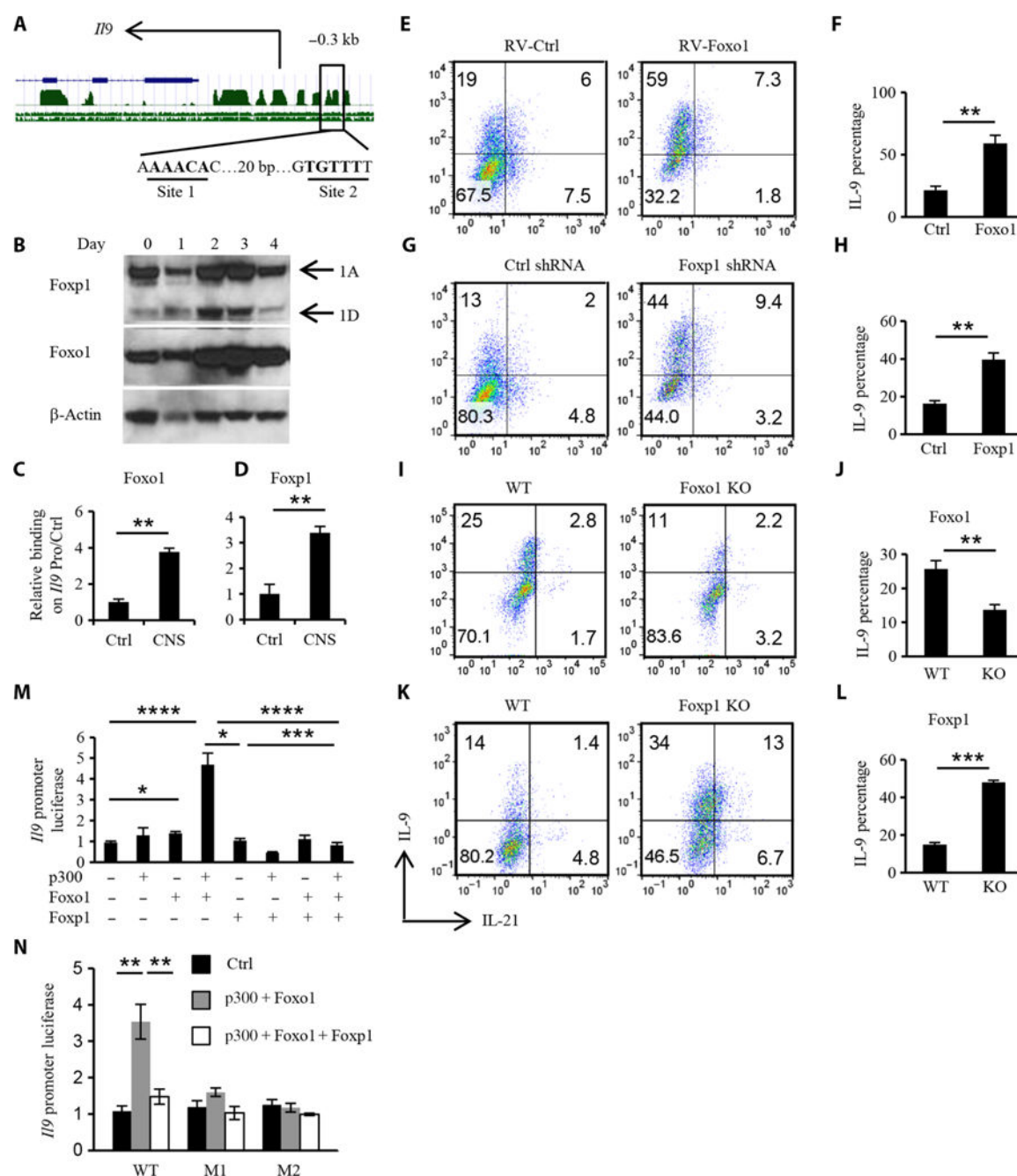


Fig. 5. Reciprocal roles for Foxp1 and Foxo1 in T_H9 cell differentiation

(A) Predicted Forkhead box transcription factor-binding sites on the *Il9* promoter. Green peaks represent the conserved regions. The blue line represents the *Il9* gene. Site 1 and site 2 are two predicted binding sites for Forkhead box transcription factors. bp, base pair. (B) Western blotting analysis of the abundances of Foxo1 and Foxp1 during T_H9 cell differentiation over time. 1A, Foxp1A; 1D, Foxp1D. (C and D) ChIP analysis of the binding of Foxo1 and Foxp1 to the *Il9* promoter in naïve OT-II $CD4^+$ T cells. Data were normalized to the *Il9* promoter control region. CNS, conserved noncoding sequence. (E and F) Naïve OT-II $CD4^+$ T cells were cultured under the T_H9 conditions for 24 hours, infected with

control or mFoxo1 retrovirus (RV) in the presence of polybrene (10 μ g/ml), and cultured for another 3 days under T_H9 conditions. The cultured T_H9 cells were then analyzed by flow cytometry to detect IL-9 and IL-21 in gated GFP⁺ (green fluorescent protein–positive) cells. **(G and H)** Preactivated CD4⁺ T cells were infected with control or Foxp1 shRNA (short hairpin RNA) lentivirus and differentiated for 4 days. Differentiated T_H9 cells were analyzed by flow cytometry to detect IL-9 and IL-21 in gated GFP⁺ cells. **(I and J)** Naïve CD4⁺ T cells were isolated from tamoxifen-treated wild-type (WT) and Foxo^{F/F} ERT2Cre mice and cultured under T_H9 conditions. Total differentiated T_H9 cells were analyzed by flow cytometry to detect IL-9 and IL-21. KO, knockout. **(K and L)** Effect of Foxp1 deficiency on T_H9 cell differentiation. WT and Foxp1^{F/F} ERT2Cre mice were treated with tamoxifen, and then isolated naïve CD4⁺ T cells were cultured under T_H9 cell–differentiating conditions before total cells were analyzed by flow cytometry to detect IL-9 and IL-21. **(M)** Luciferase activity of the *Il9* promoter combined with indicated factors to show the synergistic effect of Foxo1 and p300 and the inhibitory effect of Foxp1 on Foxo1-induced *Il9* transcription. **(N)** Mutant *Il9* promoters for site 1 (from AAACA to GAGTC, M1) and site 2 (from TGTTT to CCGGC, M2) were synthesized as indicated, and luciferase activity was analyzed to verify the specific binding locus of Foxo1 and Foxp1. Black column, control plasmids; gray column, p300 and Foxo1 plasmids; white column, p300, Foxo1, and Foxp1 plasmids. Data in (B) to (N) are from three independent experiments and are means \pm SD. * P < 0.05, ** P < 0.01, *** P < 0.001, **** P < 0.0001.

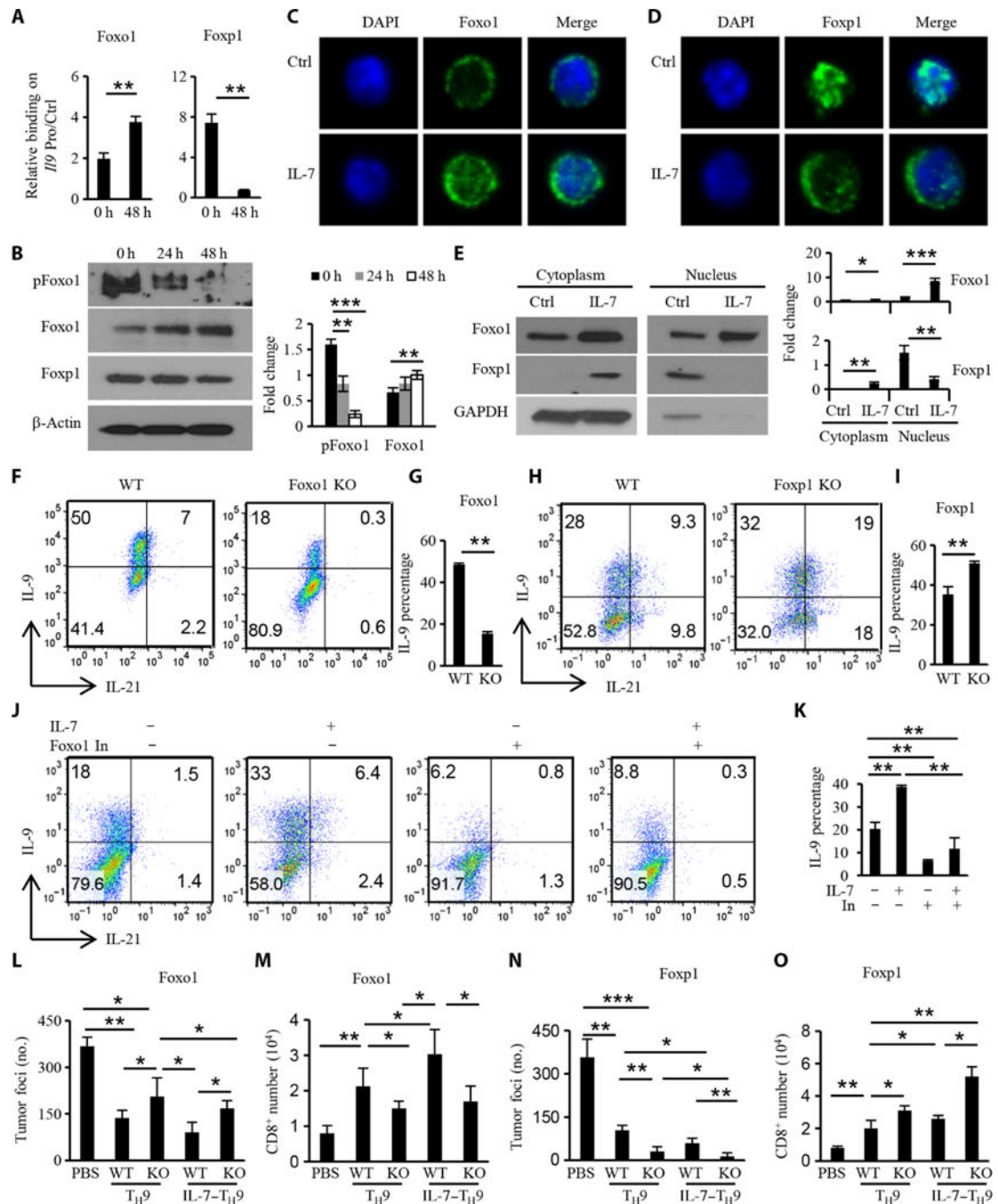


Fig. 6. Reciprocal roles for Foxo1 and Foxp1 in regulating the differentiation of IL-7-T_H9 cells and their antitumor activity

(A) ChIP analysis showing the effect of IL-7 on the binding of Foxp1 and Foxo1 to the *Il9* promoter at 48 hours. Data were normalized to the *Il9* promoter control region. (B) Western blotting analysis of the abundances of pFoxo1, Foxo1, and Foxp1 after treatment with IL-7 for the indicated times. (C and D) Effect of IL-7 on the localization of Foxo1 (C) or Foxp1 (D) in T cells after 48 hours of treatment. (E) Left: CD4⁺ T cells with or without IL-7 treatment were fractionated to generate nuclear and cytoplasmic compartments that were

then analyzed by Western blotting to detect Foxo1 and Foxp1. Right: Densitometric analysis of the indicated bands. GAPDH, glyceraldehyde-3-phosphate dehydrogenase. (F to I) Naïve CD4⁺ T cells that were untreated or were treated with IL-7 for 2 days were then stained with primary antibodies for Foxo1 and Foxp1, which was followed by incubation with FITC (fluorescein isothiocyanate)-labeled secondary antibody and DAPI (4',6-diamidino-2-phenylindole). WT and Foxo1-knockout (F and G) or WT and Foxp1-knockout (H and I) naïve CD4⁺ T cells, pretreated with IL-7 for 2 days, were cultured under T_H9 conditions for 4 days and then analyzed by flow cytometry. (J and K) Naïve CD4⁺ T cells or IL-7-pretreated CD4⁺ T cells were cultured under T_H9 conditions with or without a Foxo inhibitor (100 nM) for 4 days and then were analyzed by flow cytometry. (L to O) Effect of Foxo1 (L) or Foxp1 (N) on the IL-7-enhanced antitumor function of T_H9 cells. WT and Foxo1^{F/F} OT-II ERT2Cre or WT and Foxp1^{F/F} OT-II ERT2Cre mice were treated with tamoxifen before CD4⁺ T cells were isolated, left untreated or pretreated with IL-7, and then polarized under T_H9 conditions. The antitumor activity of the different T_H9 cells was detected in the therapeutic model as shown in Fig. 2H. Mice were sacrificed on day 14 to detect lung tumor foci. (M and O) Numbers of host CD8⁺ T cells in mouse lungs for the indicated treatments. Data in (A) to (O) are from three independent experiments and, where applicable, are presented as means ± SD. **P* < 0.05, ***P* < 0.01, ****P* < 0.001.